Available online at www.sciencedirect.com
SCIENCE DIRECT®
Journal of the European Ceramic Society 24 (2004) 3841–3848
www.elsevier.com/locate/jeurceramsoc

Predicting processing-sintering-related properties of mullite–alumina ceramic bodies based on Al-rich anodising sludge by impedance spectroscopy

M. J. Ribeiro [a], J. C. C. Abrantes [a], J. M. Ferreira [b], J. A. Labrincha [b,*]

[a] *ESTG, Polytechnique Institute of Viana do Castelo, 4900 Viana do Castelo, Portugal*
[b] *Ceramics and Glass Engineering Department, CICECO, University of Aveiro, 3810-193 Aveiro, Portugal*

Received 11 June 2003; received in revised form 11 December 2003; accepted 20 December 2003

Available online 10 May 2004

Abstract

Al-rich sludge produced from industrial anodising and surface treatment processes has been tested in the fabrication of mullite/alumina-based refractory/electrical insulating materials, by dry pressing and extrusion. Different compositions were prepared by using sub-products or common natural silica-containing materials, like ball clay, kaolin and/or diatomite. Ultimate properties are dependent on the shaping method and sintering schedule, since both steps strongly affect the microstructural evolution and crystalline phase formation, which in turn determine the performance of the sintered bodies. The response of sintered bodies to impedance spectroscopy was studied and revealed interesting microstructure–electrical relationships, enabling the use of this technique to predict the processing-sintering-related properties.

Keywords: Al_2O_3; Mullite; Waste materials; Electrical properties; Microstructural development; Impedance spectroscopy

1. Introduction

In traditional ceramic production, the shaping process adopted varies according to practical reasons: the geometry and shape complexity of the desired product, the facilities and equipment available, or the scale of productivity. It is known that different shaping techniques influence microstructural development during sintering and lead to different ultimate material properties.[1]

The most common shaping processes used for traditional ceramic products are: (i) *Dry pressing* (both unidirectional and isostatic); (ii) *Plastic forming* (extrusion, manual pressing, jiggering, usually from previously de-aired and extruded ceramic pastes); (iii) *Slip casting* (using mostly porous plaster moulds); (iv) *Pressure casting* (using plaster moulds or preferably polymeric moulds).

Normally, natural and pre-treated raw materials are used but in recent years growing efforts have been made in order to reuse industrial wastes, not only as minor additives but also as major components in traditional or technical ceramics.[2–4] As an example, the recycling of Al-rich anodising sludge as a major component for mullite or alumina refractory bodies has been studied.[5–7] Full characterisation and specification of the pre-treatment needs of Al-rich sludge, and its mixture with natural components, such as clays and kaolin has been examined, in order to obtain sintered compositions.[8,9] The refractoriness and electrical insulating characteristics of mullite-based materials are well-documented and several types of applications have been implemented.[10,11]

In addition to the preparation/shaping conditions, the sintering process is significant in determining the microstructural evolution and the final properties of the sintered bodies.[12] The sintering process is normally studied by using dilatometry or microscopy, but electrical impedance spectroscopy has also been recently tried for the same purpose, since the contributions of grains, grain boundaries, pores and other morphological aspects can be discriminated.[13,14] Accordingly, impedance spectroscopy has been used as an important tool in several different situations: (i) sintering and characterisation of clay-based dry-pressed bodies;[15,16] (ii) crack formation in materials, such as TZP;[13,14] (iii) corrosion caused by glass penetration into the YSZ-based

* Corresponding author. Tel.: +351-234370250; +351-234425300.
E-mail address: jal@cv.ua.pt (J.A. Labrincha).

0955-2219/$ – see front matter © 2004 Elsevier Ltd. All rights reserved.
doi:10.1016/j.jeurceramsoc.2003.12.026

oxygen sensors used in glass-making furnaces;[17,18] (iv) curing of cements;[19] and (v) devitrification of glazes.[20]

In the current work, impedance spectroscopy is used for the electrical characterisation of mullite-based materials constituted mainly by Al-anodising sludge in an attempt to correlate the processing and sintering-induced morphological changes with electrical behaviour.

2. Experimental procedure

The formulations used in the present work include an Al-rich sludge derived from the wastewater treatment unit of an aluminium anodising or surface coating industrial plant (Extrusal S.A., Aveiro, Portugal), as the main component; a plastic ball clay (BM-8, Barracão-Leiria, Portugal); a kaolin (Mibal-B, Barqueiros, Portugal); and pre-calcined (600 °C) diatomite (Sociedade Anglo-Portuguesa de Diatomites, Óbidos, Portugal). The Al-rich sludge was used as received (water content ≈ 85 wt.%), or after calcination (1400 °C, 2 h). The full characterization of the raw materials is given elsewhere.[5,6] Two different formulations were prepared (see Table 1) in order to produce mullite (42Al-S) or alumina-based materials (100Al-S).

Two different processing routes were used: (i) dry pressing, (ii) extrusion. The adjustment and control of processing conditions is described elsewhere.[7] Samples were sintered at different temperatures (1250–1650 °C) and microstructural changes were evaluated by SEM/EDS (Hitachi, S4100) after etching with a 5 (v/v) HF solution for 2–5 min. Stereological measurements[21] were conducted in order to evaluate the average grain size and the volumetric ratio between mullite and glassy phases. The main mineralogical phases present were detected by XRD (Rigaku Denk Co.). Real and apparent densities were also estimated, by H_2O pycnometer and Hg-immersion Archimedes method, respectively.

Table 1
Tested batch formulations (wt.%)

Composition	Al-sludge	Kaolin	Ball clay	Diatomite
42Al-S	42[a]	15	15	28
100Al-S	100[b]	–	–	–

[a] Calcined (1400 °C for 2 h)
[b] Mixture (50:50 wt.%) of wet (as-received) and calcined sludge.

Samples were electroded with porous Pt and their electrical behaviour was studied by impedance spectroscopy. Measurements were conducted between 200 and 1250 °C in the experimental setup represented in Fig. 1, using an Hewlett-Packard 4284A bridge and changing the frequency between 20 and 10^6 Hz. Fitting and interpretation of curves was done by using a specific routine program.[22] The electrical response of sintered bodies was then correlated with microstructural and crystalline phase evolutions in order to evaluate the ability of impedance spectroscopy to predict processing-sintering-related properties.

3. Results and discussion

Table 2 shows the evolution of the real and apparent densities of samples with sintering temperature. The main phases detected are also reported. The results clearly show that densification of 42Al-S composition starts earlier than that of 100Al-S, as expected from the comparison of the major phases in each system, respectively, mullite and alumina. It can be seen that although the apparent density shows an increasing trend with increasing temperature, particularly in the case of the 100Al-S composition, the maximum values of real density are achieved at 1250 °C, followed by a fall and then rise at higher temperatures. In the lower temperature range (1250–1350 °C) the denser precursors (e.g. alumina, quartz) are still present, which then transform to produce less dense phases such as mullite and crystoballite (in

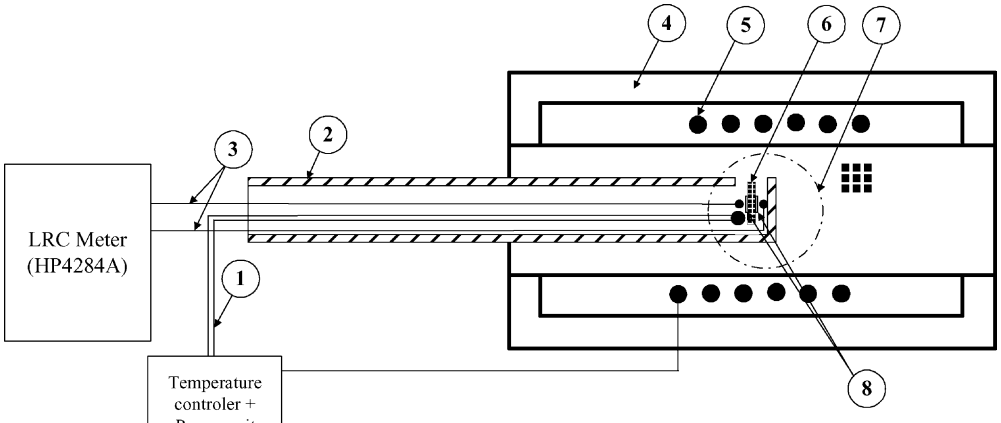

Fig. 1. Schematic view of impedance spectroscopy apparatus.

Table 2
Real and apparent densities of samples processed by different methods and sintered at different temperatures

Composition	Temperature (°C)	Shaping method	Apparent density (g/cm^3)	Real density (g/cm^3)	Main phases
42Al-S	1250	Dry pressing	2.05	–[a]	a, q, c, m
	1350		2.17	–[a]	a, q, c, m
	1450		2.13	–[a]	m
	1550		2.23	–[a]	m
	1650		2.50	–[a]	m
	1250	Extrusion	2.36	3.16	a, q, c, m
	1350		2.46	2.96	a, q, c, m
	1450		2.20	2.66	m
	1550		2.37	2.77	m
	1650		2.57	2.78	m
100Al-S	1250	Dry pressing	1.03	–[a]	s, a
	1350		1.39	–[a]	s, a
	1450		1.95	–[a]	a, b
	1550		2.70	–[a]	a, b
	1650		3.29	–[a]	a, b
	1250	Extrusion	1.04	3.70	s, a
	1350		1.32	3.71	s, a
	1450		1.96	3.66	a, b
	1550		2.72	3.59	a, b
	1650		3.34	3.61	a, b

Main phases are also given: a: α-alumina; q: quartz; c: cristoballite; m: mullite; b: β-alumina; s: $MgAl_2O_4$.
[a] These values are equal to those of the extruded samples.

the case of 42Al-S), and β-alumina (for 100Al-S). The effects of shaping method on green density and on sintering ability have been already discussed in a previous work.[7] The presence of salts gives rise to the occurrence of short range hydration forces among particles in the extruding pastes that act as a lubricant, enhancing the packing efficiency.[23] However, differences are not very strong, especially in the case of the 100Al-S composition. The evolution of phase formation seems also to be independent of the processing technique.

Fig. 2 shows typical impedance spectra for 42Al-S pressed samples that were sintered at different temperatures. Typical values of relaxation frequency (f_r) of the response arc might give a good indication of the nature of the main contribution, e.g. from the grains or grain boundaries/intergranular phases.[17,18] In general, high values are ascribed to the intragranular contribution. Despite the presence of two dominant phases (crystalline mullite and glass), all samples show a single-arc response very slightly depressed ($n > 0.97$, while a centred semicircle shows $n = 1$) attributed to dominant contribution of intragranular phenomena, as denoted by the high relaxation frequency values (see Fig. 3). As expected, resistivity tends to decrease with increasing sintering

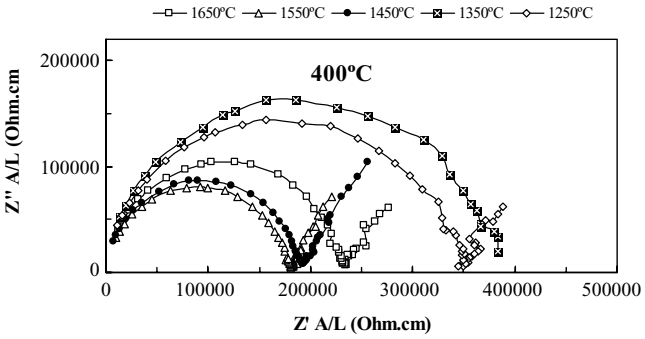

Fig. 2. Impedance spectra of 42Al-S pressed bodies sintered at different temperatures obtained at 400 °C.

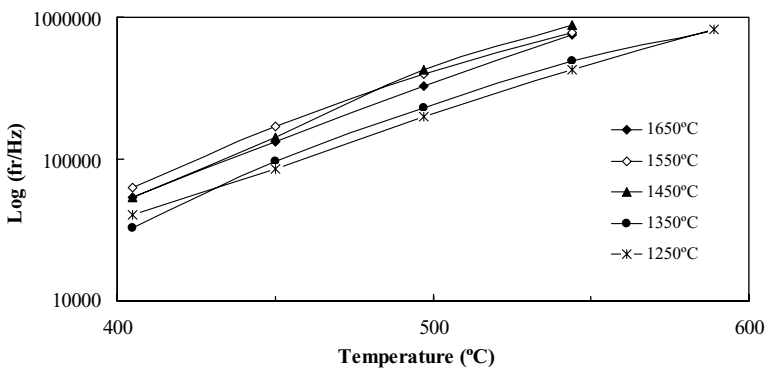

Fig. 3. Evolution of typical relaxation frequency of response arcs with measuring temperature of 42Al-S pressed samples sintered at different temperatures.

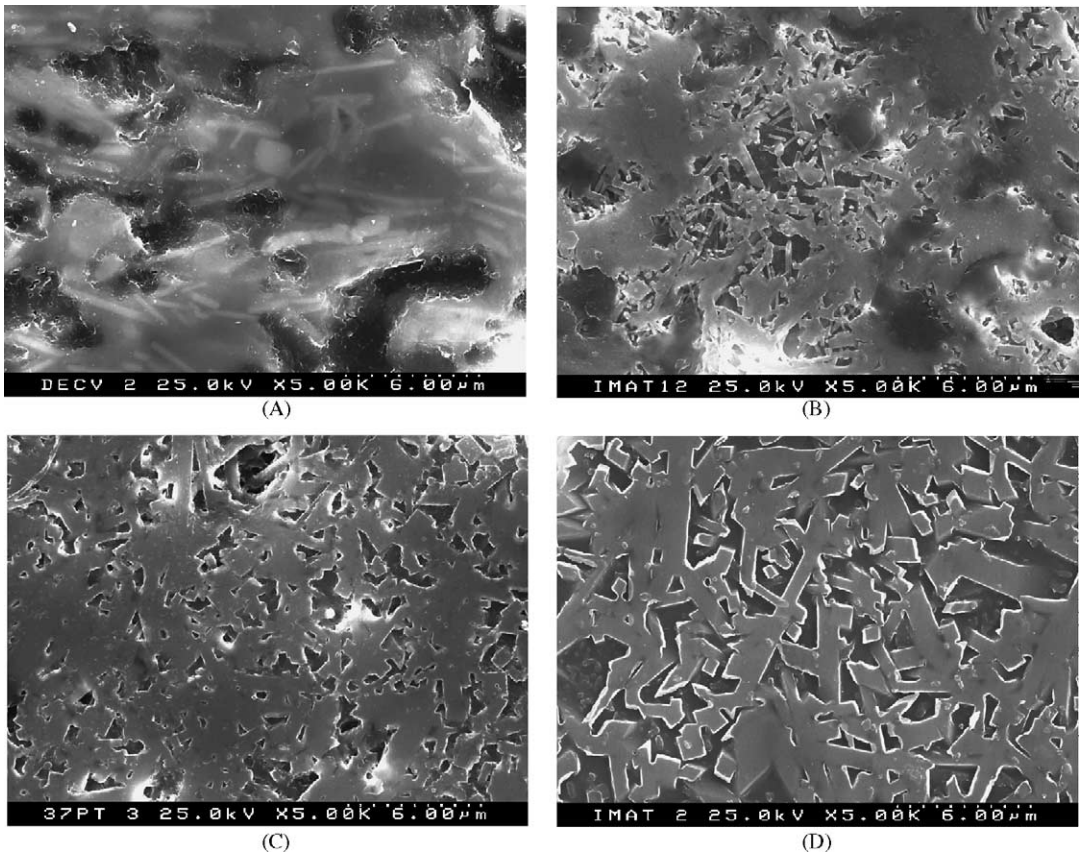

Fig. 4. Microstructures of 42Al-S pressed samples sintered at different temperatures: (A) 1350 °C; (B) 1450 °C; (C) 1550 °C; (D) 1650 °C. Pores correspond to larger voids, while the intergranular region is covered by the glassy phase, being mostly removed by chemical etching.

temperature as a consequence of the common densification process and pores' suppression (see Fig. 4). This evolution is intensified for samples that were fired between 1350 and 1450 °C, where the sintering process is more intense. Significant changes in the main crystalline phases formed also occur at this stage, with complete elimination of precursors, such as alumina, cristoballite, and quartz.[7,24] Above 1550 °C, the resistivity evolution tends to be reversed, with samples sintered at 1650 °C being relatively less conductive. At this temperature, the densification process is almost complete (see Fig. 4) and further heating will mainly cause the grain size enlargement. The percolation pathways through the glassy phase tend to decrease and an improvement of the volumetric solids (mullite) fraction might also occur, which constitutes the most resistive component if compared with the glassy phase.

Fig. 5 shows typical impedance spectra for 100Al-S pressed samples that were sintered at different temperatures. Due to its higher electrical resistance, curves were determined at higher temperatures (above 700 °C). Apparently, one single arc is again visible that tends to be more depressed than in 42Al-S composition despite the lower relative amount of glassy phase (see Fig. 6). This higher response dispersion is related with the presence of impurities or secondary phases, such as β-alumina.[5] The simultaneous presence of this phase tends to give another arc, but probably its typical relaxation frequency is similar to that of α-Al_2O_3 and then deconvolution by common fitting routines is difficult. From 1250 to 1350 °C, densification by pores suppression is responsible for the decreasing resistivity. At this stage, the formation of alumina is very incipient and decomposition reactions are still occurring.[6] Above this point, α-alumina formation and its grain growth clearly dominates the conductivity evolution that continuously decreases from 1450 to 1650 °C. The strong jump is from 1550 to 1650 °C,

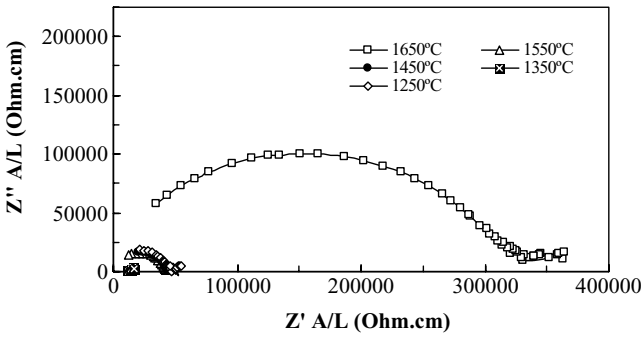

Fig. 5. Impedance spectra measured at 900 °C of 100Al-S pressed bodies sintered at different temperatures.

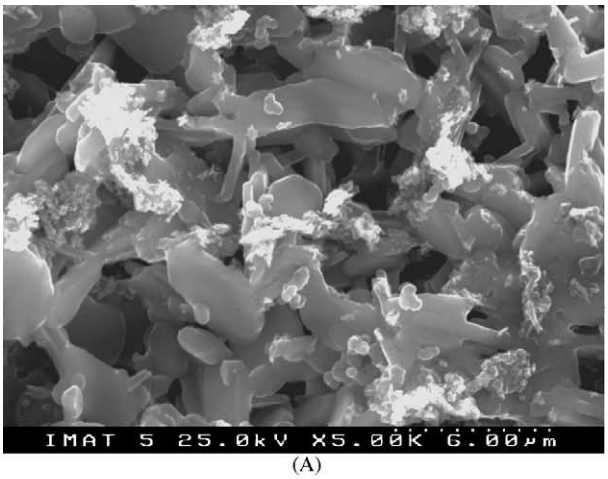

Fig. 6. Microstructures of 100Al-S pressed samples sintered at different temperatures: (A) 1450 °C; (B) 1550 °C; (C) 1650 °C. Pores correspond to larger voids, while the intergranular region was covered by the glassy phase, which was mostly removed by chemical etching.

as shown in the Arrhenius-type representation of Fig. 7. Since no abundant glassy phase formation is observed (estimated under 5 vol.%), the volume ratio between grains and grain boundaries or voids is the key microstructural influent parameter, being the grains the more resistive component.

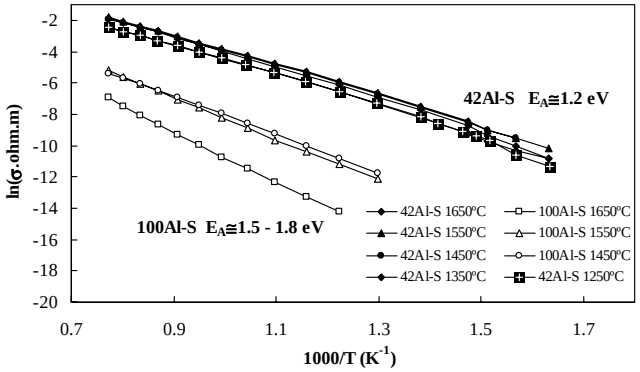

Fig. 7. Arrhenius-type plots of 42Al-S and 100Al-S pressed samples fired at different temperatures.

Fig. 8 shows the evolution of the relaxation frequency with the measuring temperature for 100Al-S samples sintered at different temperatures. The evolution is somewhat concordant with resistivity changes ($\omega_r = 1/(RC)$, being C almost constant with temperature changes) in the sense that after an increase from 1250 to 1350 °C a monotonous decrease is then observed with increasing sintering temperature. Similar observations were noticed for pure alumina commercial samples (Alcoa CT3000), also tested for comparison purposes. In the composition 42Al-S, the most significant change occurs from 1350 to 1450 °C, in accordance with previous microstructural and compositional transitions.

Fig. 7 also compares the electrical conductivity of sintered 42Al-S and 100Al-S samples. For 42Al-S samples the activation energy (E_A) is slightly higher than 1.2 eV, which is typical of mullite-based materials.[25] The effect of the processing technique was found irrelevant. Values for 100Al-S bodies are expectably higher (around 1.7 eV) than for 42Al-S, but still clearly lower than typical values for pure alumina (around 3 eV). This difference is a clear indication of the relevant role of impurities. The presence of the ionic conductor, β-alumina as a minor phase ($E_A \approx 0.15$ eV) also accounts for these results.

Microstructural changes with time at high temperatures were also evaluated by impedance measurements of samples fired at 1650 and 1550 °C, for 42Al-S and 100Al-S, respec-

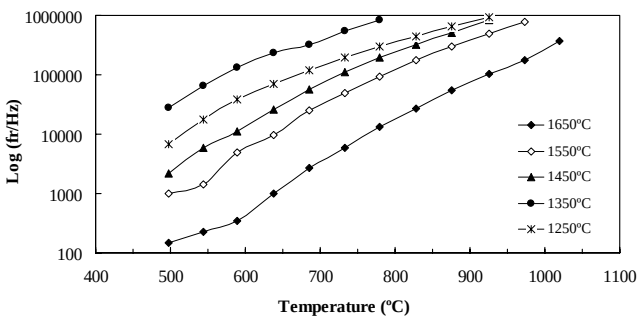

Fig. 8. Evolution of the relaxation frequency with the measuring temperature for 100Al-S pressed samples sintered at different temperatures.

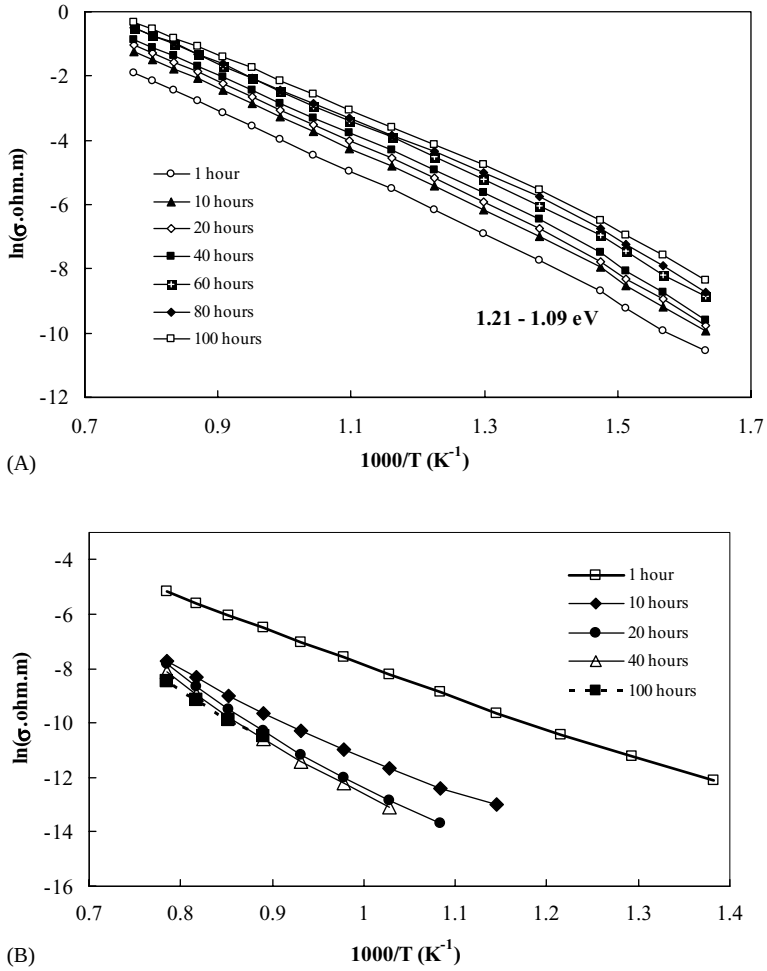

Fig. 9. Arrhenius-type plots of the conductivity of pressed samples sintered during different (dwell) times: (A) 42Al-S, 1650 °C; (B) 100Al-S, 1550 °C.

tively, during different periods. Fig. 9 shows the evolution of conductivity in Arrhenius-type plots. For 42Al-S samples (Fig. 9A) the increasing of conductivity with dwell time was somewhat unexpected taking into account the predicted increasing of grain size with time. Stereological determinations of the relevant morphological features were then evaluated as an attempt to clarify this apparent contradiction (Table 3). As can be seen, the mean grain size of mullite tends to increase with increasing exposure time, from 1.75 to 5.43 μm, for 1 and 80 h, respectively. However, the volumetric fraction of mullite (and the ratio crystalline/vitreous phase) tends to decrease as well for longer dwell times and have the dominant role in the electrical behaviour. We should remind that in this system the crystalline phase (mullite) is expectably more resistive than the glassy phase, which tends to concentrate fluxing/active elements such as alkalines. Easy pathways for charge transport are obtained when a complete interconnection of the vitreous phase is obtained, corresponding to a microstructure in which grains are completed surrounded by the glassy material without direct contacts between them. In that sense, f_r increasing is again coherent. For 100Al-S samples (Fig. 10B), the evolution of

Table 3
Microstructural relevant parameters for 42Al-S pressed samples fired at 1650 °C during different (dwell) times

Time at 1650 °C (h)	Percent mullite	Vol.% vitreous phase	Mullite/vitreous phase	Average grain size (μm)	f_r at 300 °C (Hz)
1	78.1	21.9	3.56	1.75	2.63×10^4
10	68.4	31.6	2.16	2.22	7.90×10^4
20	66.7	33.3	2.00	2.64	1.12×10^5
40	64.4	35.6	1.81	3.56	1.29×10^5
60	62.7	37.3	1.68	4.51	2.59×10^5
80	60.5	39.5	1.53	5.43	3.73×10^5
100	60.2	39.8	1.51	6.33	3.40×10^5

Typical relaxation frequency of the impedance response arc at 300 °C is also given.

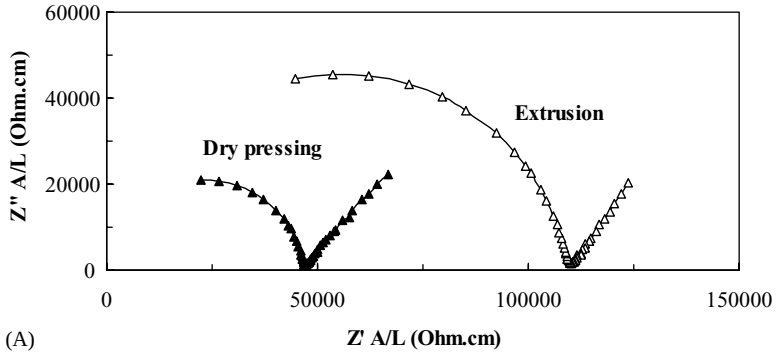

(A)

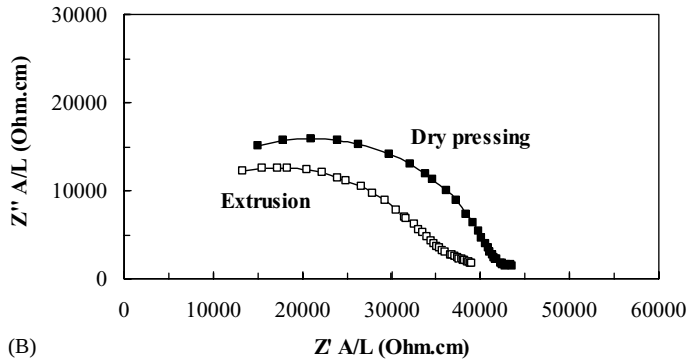

(B)

Fig. 10. Electrical response of sintered samples processed by different techniques (pressing vs. extrusion): (A) 42Al-S, 1650 °C measured at 500 °C; (B) 100Al-S, 1550 °C measured at 900 °C.

conductivity with increasing dwell time is the opposite, and now a monotonous decrease is observed. This behaviour is certainly related with the grain size enlargement of the alumina (resistive) phase, which is the dominant microstructural feature, and with the minoritary presence of a glassy phase.

Fig. 10 compares the electrical response of samples processed by different techniques. 42Al-S extruded bodies are clearly more resistive (Fig. 10A), as a consequence of the larger average size of grains and lower relative amount of glassy phase (compare Figs. 4 and 11A). Differences are expectably less pronounced for 100Al-S composition (Fig. 10B) since the amount of liquid phase formed is much smaller (Fig. 11B) and the densification degree of samples is very similar (see Table 2), irrespectively to the processing technique.

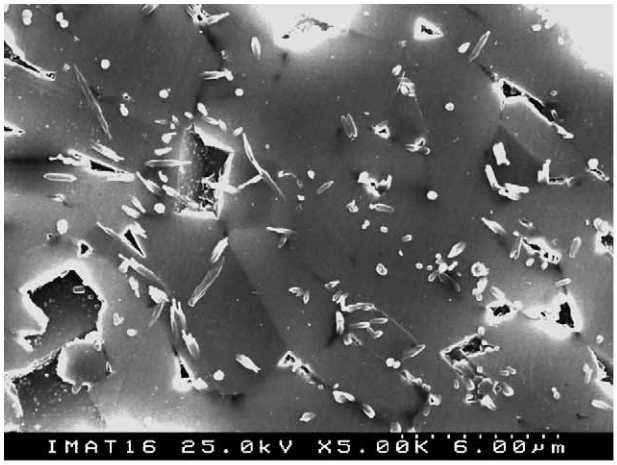

(A)

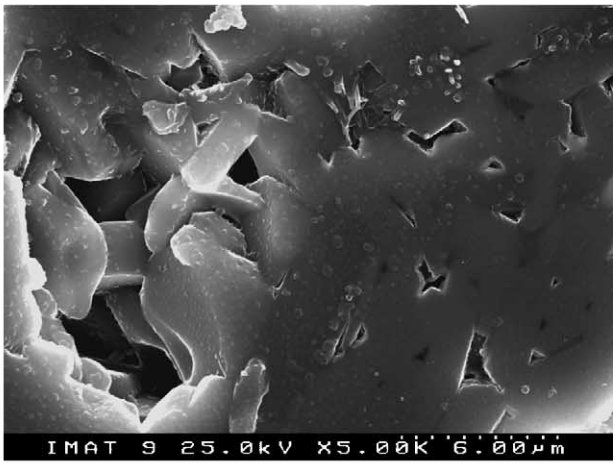

(B)

Fig. 11. Typical microstructures of samples processed by extrusion: (A) 42Al-S sintered at 1650 °C; (B) 100Al-S sintered at 1650 °C.

4. Conclusions

Recycled Al-sludge containing formulations present interesting insulating characteristics, somewhat comparable to those of mullite or alumina-based materials obtained from natural or chemical reagents. The estimated values of the activation energy for the electrical conductivity of each waste-based composition also agree reasonably well with those of corresponding pure materials. The impedance spectroscopy also proved to be a useful auxiliary technique to study the sintering process enabling to better understand the relationships between electrical behaviour and microstructural details, at least from a qualitative point of view. Changes of the average grain size and crystalline/glassy volumetric ratio during sintering were found to be the relevant morphological parameters that affect the ultimate electrical behaviour of the samples. Despite the manipulation of several variables, the role of the dominant ones was evidenced by the evaluation of impedance arcs. Further analyses should be conducted on the role of each specific variable, as an attempt to quantify some of the revealed tendencies.

Acknowledgements

Financial support from FCT (Portuguese Foundation for Science and Technology) and PRODEP 3 is greatly appreciated.

References

1. Brook, R. J., *Concise Encyclopedia of Advanced Ceramic Materials*. Pergamon Press, 1991.
2. Pereira, D. A., Couto, D. M. and Labrincha, J. A., Incorporation of aluminum-rich residues in refractory bricks. *CFI—Ceram. Forum Int.* 2000, **77**(7), 21–25.
3. Martelon, E., Jarrige, J., Ribeiro, M. J., Ferreira, J. M. and Labrincha, J. A., New clay-based ceramic formulations containing different solid wastes. *Ind. Ceram.* 2000, **20**(2), 71–76.
4. Couto, D. M. S., Labrincha, J. A., Silva, R. F., Guise, L. and Castro, F., Attempts of incorporation of metal plating sludges in ceramic products. *Ind. Ceram.* 2001, **21**(3), 163–168.
5. Tulyaganov, D. U., Olhero, S. M. H., Ribeiro, M. J., Ferreira, J. M. F. and Labrincha, J. A., Mullite-alumina refractory ceramics obtained from mixtures of natural common materials and recycled Al-rich anodizing sludge. *J. Mat. Synt. Proc.* 2002, **10**(6), 311–318.
6. Ribeiro, M. J., Tulyaganov, D. U., Ferreira, J. M. F. and Labrincha, J. A., Recycling of Al-rich industrial sludge in refractory ceramic pressed bodies. *Ceram. Int.* 2002, **28**(3), 319–326.
7. Ribeiro, M. J., Tulyaganov, D. U., Labrincha, J. A. and Ferreira, J. M. F., Production of Al-rich sludge-containing bodies by different shaping techniques. *J. Mat. Processing Tech*., in press.
8. Seabra, A. M., Pereira, D. A., Bóia, C. S. and Labrincha, J. A., Pre-treatment needs for the recycling of Al-rich anodizing sludge as a ceramic raw material. In *Proceedings of 1st Latin American Clay Conference* (*Vol 2*), ed. C. S. Gomes. Portuguese Clay Society, pp. 176–181.
9. Nunes, P., Ribeiro, M. J., Ferreira, J. M. F., Bóia, C. S. and Labrincha, J. A., Mullite-based materials obtained from industrial wastes and natural sub-products. In *Proceedings of the TMS Fall Meeting on Recycling and Waste Treatment in Mineral and Metal Processing: Technical and Economic Aspects* (*Vol 2*), ed. B. Bjorkman, C. Samuelsson and J. Wikstrom. Lulea, Sweden, 2002, pp. 359–368.
10. Aksay, I. A., Dabbs, D. M. and Sarikaya, M., Mullite for structural, electronic and optical applications. *J. Am. Ceram. Soc.* 1991, **74**(10), 2343–2358.
11. Mizuno, M., Microstructure, microchemistry, and flexural strength of mullite ceramics. *J. Am. Ceram. Soc.* 1991, **74**(12), 3017–3022.
12. Kara, F., Turan, S., Little, J. A. and Knowles, K. M., Microstructural characterization pf reactively sintered mullites. *J. Am. Ceram. Soc.* 2000, **83**(2), 369–376.
13. Dessemond, L., Guindet, J., Hammou, A. and Kleitz, M., Impedancemetric characterization of cracks and pores in zirconia based materials. In *Proceedings of the Second International Symposium on Solid Oxide Ful Cells*, ed. F. Grosz, P. Zegers, S. C. Singhal and O. Yamamoto. Office for Official Publications of European Communities, Bruxelles, 1991, pp. 409–416.
14. Kleitz, M., Pescher, C. and Dessemond, L., Impedance Spectroscopy of microstructure defects and crack characterisation. In *Science and Technology of Zirconia V*, ed. S. P. S. Badwall., M. J. Bannioster and R. H. J. Hannink. Technomic Publ. Co., Inc., PA, 1993, pp. 593–608.
15. Vancaster, N., Moortgat, G. and Cambier, F., Characterisation of pressed clay products by electrochemical impedance spectroscopy. *Tile Brick Int.* 2000, **16**(5), 322–327.
16. Wang, X. and Xiao, P., Characterisation of clay sintering process using impedance spectroscopy. *J. Eur. Ceram. Soc.* 2002, **22**, 471–478.
17. Rodrigues, C. M. S., Labrincha, J. A. and Marques, F. M. B., Monitoring of corrosion of YSZ by impedance spectroscopy. *J. Eur. Ceram Soc.* 1998, **18**, 95–104.
18. Rodrigues, C. M. S., Labrincha, J. A. and Marques, F. M. B., Study of yttria stabilized zirconia/glass composites by impedance spectroscopy. *J. Electrochem. Soc.* 1997, **144**(12), 4303–4309.
19. Christensen, B. J., Coverdale, R. T., Olson, R. A., Ford, S. J., Garboczi, E. J., Jennings, H. M. *et al.*, Impedance spectroscopy of hydrating cement-based materials: measurement, interpretation, and application. *J. Am. Ceram. Soc.* 1994, **77**(11), 2789–2802.
20. MacDonald, J. R. and Francheschetti, D., *Impedance Spectroscopy Emphasing Solid Materials and Systems*. Wiley-Interscience, 1988, p. 90.
21. Underwood, E. E., *Quantitative Stereology*. Addison-Wesley, Georgia, 1970.
22. Abrantes, J. C. C. and Frade, J. R., Computing tools for quick inspection and interpretation of impedance spectra. In *OSSEP/ESF Workshop, Ionic and Mixed Conductors: Methods and Processes*. Aveiro, Portugal, April 10–12, 2003.
23. Lange, F. F., Powder processing science and technology for increased reliability. *J. Am. Ceram. Soc.* 1989, **72**, 3–15.
24. Chen, C. Y., Lan, G. S. and Tuan, W. H., Preparation of mullite by the reaction sintering of kaolinite and alumina. *J. Eur. Ceram. Soc.* 2000, **20**, 2519–2525.
25. Chaudhuri, S. P., Patra, S. K. and Chakraborty, A. K., Electrical resistivity of transition metal ion doped mullite. *J. Eur. Ceram. Soc.* 1999, **19**, 2941–2950.